Liu et al. *Zool. Res.* 2025, 46(5): 996−1008
https://doi.org/10.24272/j.issn.2095-8137.2025.086
https://cstr.cn/32248.14.zr.2025.086

ZR | Zoological Research

Article Open Access

Dopaminergic neurons in the dorsal raphe nucleus may modulate social dominance in mice

Ying-Juan Liu[1,#], Qin An[2,#], Bai-Lin Song[1,#], Jia Tian[1], Lu Ren[2], Ya-Han Sun[2], Jiao-Wen Wu[1], Jie Zhou[1], Zhi-Xiong He[2], Fa-Dao Tai[2,*], Lai-Fu Li[1,2,*]

[1] *Research Center of Henan Provincial Agricultural Biomass Resource Engineering and Technology*, *College of Life Science*, *Nanyang Normal University*, *Nanyang*, *Henan* 473061, *China*

[2] *Institute of Brain and Behavioral Sciences*, *College of Life Sciences*, *Shaanxi Normal University*, *Xi'an*, *Shaanxi* 710119, *China*

ABSTRACT

Social hierarchies are central to the organizational structure of group-living species, shaping individual physiology, behavior, and social interactions. Dopaminergic (DA) systems, particularly within the ventral tegmental area (VTA) and dorsal raphe nucleus (DR), have been linked to motivation and competitive behaviors, yet their region-specific contributions to social dominance remain insufficiently defined. This study investigated the role of VTA and DR DA neurons in regulating social dominance in sexually naïve male C57BL/6J mice. Stable hierarchies were established using the tube test, after which both dominant and subordinate mice exhibited elevated c-Fos expression within the VTA and DR. Notably, dominant mice displayed significantly greater c-Fos activation in DR DA neurons compared to subordinates. Fiber photometry revealed that DA neurons in both regions were activated during proactive push behaviors and inhibited during passive retreats, with DR neurons showing stronger activation during dominance-related actions. Chemogenetic inhibition of DR DA neurons in dominant mice reduced their social rank, whereas activation in subordinates elevated their rank. In contrast, chemogenetic modulation of VTA DA neurons had no significant effect on social dominance. Manipulation of DA neurons in both regions produced rank-dependent changes in specific anxiety-like behavioral phenotypes. These findings highlight the distinct roles of DR and VTA DA neurons in social hierarchy regulation, identifying DR DA neurons as a critical component in the modulation of social dominance.

Keywords: Social hierarchy; Dorsal raphe nucleus; Ventral tegmental area; Dopamine; Chemogenetics

INTRODUCTION

Dominance hierarchies are a defining feature of social organization in group-living animals (Qu et al., 2017), serving not only as a social framework but also as a critical regulatory mechanism that governs resource allocation and maintains group stability (Leclair & Russo, 2021). These hierarchies exert profound impacts on individual fitness, creating a marked asymmetry in welfare (Johnson et al., 2012). Dominant individuals typically secure preferential access to essential resources such as food, shelter, mating opportunities, conferring advantages for physical health and reproductive success (Uchida et al., 2022). In contrast, subordinate individuals experience chronic psychosocial stress that predisposes them to a spectrum of psychopathological and physiological disorders (Madigan & Daly, 2023). This dichotomy underscores the neurobiological significance of social hierarchy, offering insight into fundamental ethological processes while informing translational approaches to mental health disorders (Battivelli et al., 2024b; Dwortz et al., 2022).

Multiple neuromodulatory systems have been implicated in the establishment and maintenance of social hierarchies, including dopamine (DA), serotonin (5-HT), oxytocin, and steroid hormones (Janet et al., 2022; Liu et al., 2025; Zhou et al., 2018). Among these, the DA system, which is closely associated with reward and motivation, has emerged as a key modulator of competitive outcomes (Amaral et al., 2021). In rats, dopaminergic projections from the ventral tegmental area (VTA) to the nucleus accumbens (NAc) are critical determinants of victory in social competition (van der Kooij et al., 2018). Similarly, dominant nonhuman primates exhibit elevated cerebrospinal fluid concentrations of DA metabolites (Kaplan et al., 2002), and in humans, striatal dopamine D2/3

Received: 13 April 2025; Accepted: 26 May 2025; Online: 27 May 2025

Foundation items: This work was supported by the National Natural Science Foundation of China (32270529 to L.F.L.; 32270510 to F.D.T.); STI2030-Major Projects (2022ZD0205101 to F.D.T.); Natural Science Foundation of Henan Province (252300420211 to Y.J.L.), and Key Scientific Research Project of Higher Education Institutions in Henan Province (23A180001 to L.F.L.)

[#]Authors contributed equally to this work

*Corresponding authors, E-mail: taifadao@snnu.edu.cn; lilaifu@snnu.edu.cn

receptor binding is positively correlated with social status (Martinez et al., 2010).

DA neurons are primarily localized to the substantia nigra, VTA, and dorsal raphe nucleus (DR), each with distinct projection targets and functional roles. Substantia nigra DA neurons innervate the dorsal striatum and are essential for motor control (Tenchov et al., 2025). VTA DA neurons project extensively to forebrain and limbic structures, modulating emotion, motivation, memory, and reward-related behavior (Garritsen et al., 2023; Lin et al., 2021). While optogenetic activation of VTA DA neurons enhances dominance in rats in competitive contexts (Lozano-Montes et al., 2019), recent evidence indicates that dominant mice actually display reduced dopaminergic activity in the VTA (Battivelli et al., 2024b). Moreover, projections from the medial prefrontal cortex (mPFC) to the VTA have been shown to encode social defeat in mice (Choi et al., 2024). Accumulating evidence identifies DR DA neurons as a unique subpopulation with specialized projection patterns, primarily targeting the bed nucleus of the stria terminalis (BNST) and central amygdala (CeA), with functional implications in arousal modulation, memory processing, sociability, and depression-related behaviors (Cho et al., 2017; Lin et al., 2020, 2021; Matthews et al., 2016; Wang et al., 2024). Despite these associations, the role of DR DA neurons in social competition has not, to our knowledge, been systematically examined.

This study examined the contributions of DR and VTA DA neurons to the regulation of social hierarchy in mice. Post-test c-Fos expression profiles in these neuronal populations were quantified following tube test assessments in triad-housed cohorts. Real-time calcium imaging was employed to monitor neuronal activity during competitive interactions, and chemogenetic manipulations were applied to determine causal effects on social ranking. Given the established roles of the DA system in emotional regulation and social behavior (Liu et al., 2021; Torquet et al., 2018), anxiety-like behaviors and social preference were also evaluated during testing. Results revealed that DR DA neurons in dominant mice exhibited greater activation after the tube test, and bidirectional manipulation of these neurons altered dominance status. In contrast, modulation of VTA DA neuronal activity did not influence rank. These findings suggest that DR DA neurons exert a more prominent influence on social dominance than VTA DA neurons in mice. Our study provides novel insights into the neural representation of social hierarchy, which has significant implications for health and welfare.

MATERIALS AND METHODS

Animals

Sexually naïve male C57BL/6J mice (8–10 weeks old, 25–28 g) were obtained from Huaxing Experimental Animal Farm (Zhengzhou, China). Mice were housed in groups of three per cage (26 cm long×20 cm wide×14 cm high) under standard conditions (22±3°C, 12 h:12 h light/dark cycle with lights on at 0700 h) with *ad libitum* access to food and water. All experimental procedures complied with the Chinese Guidelines for Laboratory Animal Care and Use and were approved by the Nanyang Normal University Animal Ethics Committee (Protocol #202306010003). Unless otherwise indicated, experimental manipulations were restricted to dominant or subordinate mice, with intermediate-ranked mice maintained as undisturbed controls for social hierarchy assessment.

Behavioral tests

All behavioral tests were conducted between 0900h and 1400h under low-light conditions. Mice were habituated to the testing room for 30 min prior to each session. Unless indicated otherwise, the tests were video-recorded and analyzed using SuperMaze Systems (Shanghai Xinruan, China). Apparatuses were cleaned with 30% ethanol and dried with paper towels between sessions.

Tube test: Social dominance among mice was determined using the tube test (Fan et al., 2019; Li et al., 2023). The apparatus consisted of a transparent tube (30 cm long and 3.5 cm internal diameter) permitting passage of only one mouse at a time. Mice were individually trained to traverse the tube for five trials per day over three consecutive days. During the testing phase, cage-mates were trained in pairs for three additional trials and subsequently assessed in dyadic encounters using a round-robin design. Each trial began with one mouse placed at either end of the tube and allowed to meet in the middle, with the encounter ending when one mouse forced the other to retreat completely from the tube. The retreating mouse was designated the “loser”, while the advancing mouse was designated the “winner”. Trials exceeding 5 min were terminated and repeated later. Only cages with stable social hierarchies for at least four consecutive days were included in subsequent experiments. Hierarchical rank within each cage was assigned as top (rank 1), middle (rank 2), and bottom (rank 3).

Open-field test (OFT): The OFT was used to assess locomotor activity and anxiety-like behavior (Zhou et al., 2024). The apparatus consisted of an opaque plastic box (50 cm long×50 cm wide×50 cm high) with the floor virtually divided into 16 equal quadrants, with the four central quadrants defined as the central zone. During the test, each mouse was placed individually in the box and allowed to freely explore for 5 min. Time spent in the central zone and total distance traveled were recorded automatically.

Elevated plus maze test (EPM): The EPM apparatus consisted of two open arms (35 long×5 wide×1 cm high) and two closed arms (35 cm long×5 cm wide×15 cm high) extending from a central platform (5 cm long×5 cm wide). The maze was elevated 70 cm above the floor. Mice were placed on the central platform facing an open arm and allowed to freely explore for 5 min. The number of entries and time spent in each arm were recorded for analysis.

Social interaction (SI) test: Sociability was evaluated using the SI test (Wang et al., 2022), conducted in the same open-field box apparatus described above. A wire mesh cage (11 cm high×9 cm diameter) was placed in the center of one side of the box. The floor was virtually divided into an interaction zone (30 cm long×20 cm surrounding the wire cage) and non-interaction zone. The test consisted of two 5 min trials. In the first “target-absent” trial, the wire mesh cage was empty. In the second “target-present” trial, a novel C57BL/6J male mouse was placed into the wire mesh cage. Time spent in the interaction and non-interaction zones during both trials was recorded. Sociability was quantified as the SI ratio, defined as the time spent in the interaction zone during the target-present trial divided by the time spent in the interaction zone during the target-absent trial.

Immunofluorescence

One day after the completion of behavioral testing, the

animals underwent six consecutive tube test trials. Ninety minutes after the final trial, mice were euthanized with 2% sodium pentobarbital and perfused transcardially with 0.1 mol/L phosphate-buffered saline (PBS), followed by 4% paraformaldehyde (PFA). Brains were then quickly removed, post-fixed in 4% PFA for three days, and dehydrated in 15% and 30% sucrose solutions. The brains were then cut into 40-μm coronal sections using a cryostat (Leica CM1950, Germany) and mounted onto gelatin-coated glass slides. Thereafter, the sections were rinsed with PBS (5 min×3), blocked with 5% normal goat serum for 2 h at room temperature, and incubated overnight at 4°C with primary antibodies: rabbit anti-c-Fos (1:2 000, ab190289, Abcam, UK) and mouse anti-tyrosine hydroxylase (TH, a rate-limiting enzyme in DA synthesis) (1:500, sc-25269, Santa Cruz, USA). After fully washing with PBS (5 min×3), the sections were incubated for 2 h at room temperature with secondary antibodies: goat anti-rabbit conjugated with TRITC (1:400, AB_2337932, Jackson, USA) and goat anti-mouse conjugated with 488 (1:400, 115545146, Jackson, USA). All sections were then stained with DAPI at room temperature for 10 min, washed in PBS (5 min×3), and finally imaged using a ZEISS inverted fluorescence microscope Axio Observer 7 (Carl Zeiss AG, Germany). Quantification of Fos-positive and TH-positive neurons was performed on three anatomically matched sections spanning rostral to caudal regions of the mouse brain, using consistent regions of interest (ROIs) to ensure consistency. For each mouse, counts from the three sections were averaged to minimize variability. The TH/c-Fos colocalization rate was calculated by dividing the number of TH/c-Fos double-labeled cells by the number of TH-labeled cells.

Viral vectors

Adeno-associated viral (AAV) vectors used in this study included: AAV-TH-CRE-WPRE-hGH-polyA (Cat#: PT-2947, BrainVTA, China), AAV-EF1α-DIO-mCherry-WPRE-hGH-polyA (Cat#: PT-0013, BrainVTA, China), AAV-EF1α-DIO-hM3D(Gq)-mCherry-WPREs (Cat#: PT-0042, BrainVTA, China), AAV-EF1α-DIO-hM4D(Gi)-mCherry-WPREs (Cat#: PT-0043, BrainVTA, China), AAV-TH-GCaMP6s-WPRE-hGH-polyA (Cat#: PT-2148, BrainVTA, China), and AAV-TH-eGFP-WPRE-hGH-polyA (Cat#: PT-0184, BrainVTA, China). Titer values were 3–4×10^{12}/mL.

Viral injection and chemogenetic manipulations

Mice were anesthetized with isoflurane inhalation (1.5%–3.0%) and placed in a stereotaxic instrument (RWD Life Science, China). The skull was exposed, and viral vectors were stereotactically injected into the targeted sites via a 33-gauge syringe needle (Hamilton, Switzerland). Cre-expressing and DIO-AAV vectors were combined at a 1:1 volumetric ratio and injected at 100 nL/min to a total of 600 nL. The syringe was left in place for 5 min post-infusion before gradual withdrawal to prevent reflux. Mice were returned to their original cages post-surgery and left undisturbed until subsequent experiments. Target coordinates relative to bregma were: VTA: AP −3.2 mm, ML±0.5 mm, DV – 4.7 mm; DR: AP −4.0 mm, ML +0.2 mm, DV −3.3 mm. Behavioral assessments commenced three weeks after viral delivery.

For chemogenetic manipulation, clozapine-N-oxide (CNO, Cat#: CNO-01, BrainVTA, China) was dissolved with 1% dimethyl sulfoxide (DMSO), then diluted with normal saline at a final concentration of 1 mg/mL. Solutions were stored at −20°C until use. Thirty minutes before behavioral testing, mice received an intraperitoneal injection of vehicle (Veh) or CNO (0.2 mL) under brief anesthesia.

Fiber photometry

AAV-TH-GCaMP6s or control AAV-TH-eGFP was injected into the VTA or DR (500 nL per site). Three weeks post-injection, an optical fiber (core diameter: 250 μm) was implanted 0.3 mm dorsal to the injection site and secured with a screw and dental acrylic. Tube test-based dominance ranking was determined one week after implantation.

Recordings were performed using a three-color single-channel fiber photometry system (ThinkerTech, China) to monitor Ca^{2+} signals in VTA and DR DA neurons. A 470 nm laser light was used to excite and record green fluorescent signals of GCaMP6s, while the 405 nm signal was used as a control channel to correct motion artifacts. To reduce GCaMP6s bleaching, laser intensity was adjusted at the end of the optic fiber to 40 μW, and sampling frequency was set at 100 Hz.

Fiber photometry recordings followed established procedures (Zhang et al., 2022), with testing only including mice with stable hierarchical ranking. The apparatus consisted of a modified 60 cm tube equipped with two movable doors positioned 15 cm from one end. Mice were held in the tube prior to door opening to establish a baseline recording and minimize interference from human handling. Behavioral events were recorded using a side-mounted camera within the open-field box. Behavioral annotation during analysis distinguished three categories: walking alone, pushing (initiating contact by shoving the head beneath an opponent), and retreating (voluntary withdrawal or displacement, typically with head lowering) (Fan et al., 2023). Three to five bouts of each behavior were collected per mouse.

Fluorescence traces were aligned to behavioral onset, capturing 2 s before and 3 s after the start of each behavior. The 405 nm signal was subtracted from the 470 nm signal, and ΔF/F was calculated as $(F-F_0)/F_0$, where F_0 represents the baseline fluorescence signal averaged over a 1 s window between 5 s and 4 s before a specific behavioral event. Normalized area under the curve (AUC) values were calculated as the sum of fluorescence changes during the behavioral epoch divided by its duration. Subjects were excluded from analysis if postmortem examination revealed a lack of viral expression or improper fiber placement.

Data analysis

Pairwise comparisons were conducted using independent-samples or paired *t*-tests, as appropriate. Comparisons among three or more groups used one-way analysis of variance (ANOVA), while two-way repeated-measures ANOVA was used to compare multiple groups under multiple testing conditions. *Post-hoc* analyses were performed using Bonferroni correction. Rank switching rates were analyzed using Fisher's exact test. Statistical significance was set at $P<0.05$. All analyses were performed using SPSS v.22.0. Details on analysis methods and sample size are provided in the figure legends.

RESULTS

Characteristics of social hierarchies and behavioral profiles across rank groups

The tube test was employed to assess social hierarchy

formation and its stability over time in triads of male C57BL6/J mice housed together for at least one week (Figure 1A–B). By the fourth day of testing, most cohorts displayed a stable hierarchical structure (Figure 1C). A dominance score, calculated as the mean number of daily wins for each individual across rank groups, served as a quantitative index of dominance behavior. Results indicated that rank 1 mice exhibited significantly higher dominance scores compared with both rank 2 and rank 3 mice (Figure 1D) ($F_{(2,21)}$=49.650, P<0.010; rank 1 vs. rank 2, rank 1 vs. rank 3, rank 2 vs. rank 3, all P<0.010). To further examine behavioral traits associated with social rank, the OFT was used to measure exploratory activity and anxiety-like behavior, the EPM test was used to evaluate the conflict between natural fear and exploration, and the SI test was applied to assess sociability. However, no significant rank-related differences were observed across these measurements (Figure 1E: $F_{(2,21)}$=0.016, P=0.984; Figure 1F: $F_{(2,21)}$=0.064, P=0.938; Figure 1G: $F_{(2,21)}$=0.029, P=0.880; Figure 1H: $F_{(2,21)}$=0.450, P=0.643; Figure 1I: $F_{(2,21)}$=0.018, P=0.982; Figure 1J: $F_{(2,21)}$=0.109, P=0.897).

c-Fos expression in DR DA neurons is selectively elevated in dominant mice following social competition

To investigate the involvement of DA signaling in the formation and maintenance of social hierarchies, neuronal activation in the VTA and DR following social rank competition was assessed using TH and c-Fos double-labeling. A control group was included in which mice traversed the tube six times without competitive encounters prior to immunostaining. In the VTA, c-Fos expression was significantly elevated in both the dominant and subordinate mice relative to controls (Figure 2G; $F_{(2,\ 18)}$=27.620, P<0.010; dominants and subordinates vs. control, all P<0.010). However, the proportion of c-Fos-positive TH-immunoreactive (c-Fos$^+$TH$^+$) neurons did not differ significantly among groups (Figure 2H; $F_{(2,18)}$=1.499, P=0.250). In the DR, c-Fos expression was also elevated following the tube test (Figure 2I; $F_{(2,18)}$=46.3, P<0.010; dominants and subordinates vs. control, all P<0.010; dominants vs. subordinates, P=0.016). Furthermore, the proportion of c-Fos$^+$TH$^+$ neurons was markedly higher in dominant mice compared with both subordinates and controls (Figure 2J; $F_{(2,18)}$=38.24, P<0.010, subordinates and controls vs. dominants, all P<0.010, subordinates vs. control, P=0.028). TH$^+$ neurons did not differ significantly among groups in either the VTA or DR (Supplementary Figure S1; VTA: $F_{(2,18)}$=0.130, P=0.880; DR: $F_{(2,18)}$=0.240, P=0.790), indicating social rank does not alter DA synthesis capacity. Collectively, these findings demonstrate that while general neuronal activation in both the VTA and DR is associated with competitive encounters, selective recruitment of DR DA neurons is strongly linked to dominant status, suggesting a preferential role for this population in modulating social dominance.

Both VTA and DR DA neurons exhibit opposing activity patterns during competitive push and retreat behaviors

In vivo fiber photometry was applied to capture real-time DA neuronal activity during tube test competition. *Post-hoc* histological examination confirmed that approximately 75% of GCaMP6s$^+$ cells were co-labeled with TH in both the VTA and DR (Supplementary Figure S2).

During competitive encounters, GCaMP6s fluorescence in both regions increased sharply at the onset of push behaviors resulting in a win and decreased during retreat behaviors resulting in a loss (VTA: Figure 3E–G, I–K; DR: Figure 4D–F, H–J). Quantitative analysis revealed significant increases in AUC per second during push epochs but significant decreases during retreat epochs (Push: VTA, pre vs. post: $t_{(5)}$=5.175, P<0.010, Figure 3G. DR, pre vs. post: $t_{(5)}$=9.280, P<0.010, Figure 4F. Retreat: VTA, pre vs. post: $t_{(5)}$=6.699, P<0.010, Figure 3K. DR, pre vs. post: $t_{(5)}$=4.299, P<0.010, Figure 4J). Comparison between regions showed that the DR exhibited a significantly greater AUC per second than the VTA during push epochs (VTA vs. DR, $t_{(10)}$=6.063, P<0.010; Supplementary Figure S3B), although peak values did not differ significantly (VTA vs. DR, $t_{(10)}$=2.013, P=0.062; Supplementary Figure S3C). During retreat epochs, DR neurons reached significantly lower valley values than those in the VTA (VTA vs. DR, $t_{(10)}$=2.590, P=0.027; Supplementary Figure S3F), while the AUC per second displayed a similar trend without reaching significance ($t_{(10)}$=2.214, P=0.051, Supplementary Figure S3E).

No significant changes in GCaMP6s fluorescence were detected when mice traversed the tube in the absence of an opponent (VTA: Figure 3M–O; DR: Figure 4L–N. Figure 3O: $t_{(5)}$=1.069, P=0.334; Figure 4N: $t_{(5)}$=0.252, P=0.811) or when viral control mice participated in competitive trials (VTA: Figure 3H, L, P; DR: Figure 4G, K, O. Figure 3H: $t_{(5)}$=1.424, P=0.214; Figure 3L: $t_{(5)}$=1.433, P=0.211; Figure 3P: $t_{(5)}$=0.385, P=0.716; Figure 4G: $t_{(5)}$=0.036, P=0.973; Figure 4K: $t_{(5)}$=0.493, P=0.643; Figure 4O: $t_{(5)}$=1.193, P=0.286). These results confirm that the recorded GCaMP6s signals reflect genuine neuronal activity linked to competitive behaviors, rather than motion-induced artifacts.

Chemogenetic manipulation of VTA DA neurons does not alter social dominance but modulates select anxiety-like behaviors

To assess the contribution of VTA neurons to social dominance, neuronal activity was bidirectionally modulated using chemogenetics, with dominant and subordinate mice receiving VTA injections of AAV-DIO-hM3D(Gq)-mCherry+AAV-TH-CRE, AAV-DIO-hM4D(Gi)-mCherry+AAV-TH-CRE, or control AAV-DIO-mCherry+AAV-TH-CRE. Robust DREADD expression was detected in the VTA (Figure 5C), with immunohistochemical analysis showing that 74.5% of mCherry+ cells co-expressed TH (Supplementary Figure S4B). Functional validation was performed by administering CNO (1 mg/kg, intraperitoneal) and quantifying c-Fos expression 90 min later. Compared with controls, c-Fos$^+$ neurons were significantly higher in hM3D(Gq) mice and lower in hM4D(Gi) mice (Supplementary Figure S4E, F; $F_{(2,15)}$=37.320, P<0.010; hM3D(Gq) vs. Control, P<0.01, hM4D(Gi) vs. Control, P=0.017), confirming the efficacy of the viral strategy.

In the tube test, chemogenetic manipulation of VTA DA neurons produced no significant changes in dominance rank in either dominant or subordinate mice (dominance: hM3D(Gq)+Veh vs. hM3D(Gq)+CNO, rank change rate: 25%, Fisher's exact test, P=0.467, Figure 5E; hM4D(Gi)+Veh vs. hM4D(Gi)+CNO, rank change rate: 50%, Fisher's exact test, P=0.077, Figure 5F. Subordinates: hM3D(Gq)+Veh vs. hM3D(Gq)+CNO, rank change rate: 37.5%, Fisher's exact test, P=0.2, Figure 5H; hM4D(Gi)+Veh vs. hM4D(Gi)+CNO, rank change rate: 37.5%, Fisher's exact test, P=0.2, Figure 5I).

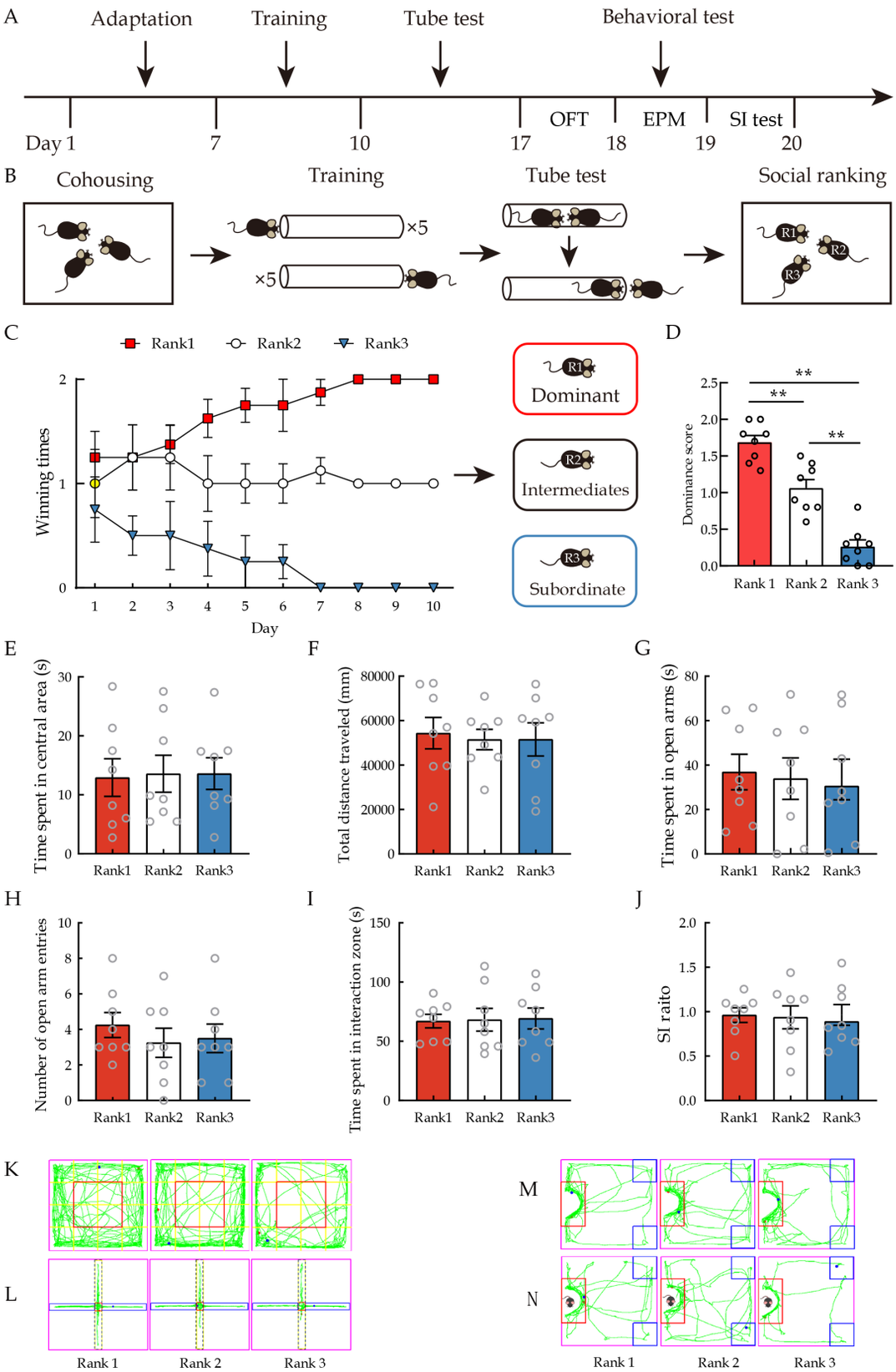

Figure 1 Social rank and behavioral performance

A: Study timeline. B: Schematic of the tube test. C: Social rank changes during training and the tube test. D: Dominance scores. Average number of wins per day across all days of the tube test is depicted for individuals categorized by rank. E, F: Time spent in the central zone and total distance traveled in OFT. G, H: Time spent in open arms and number of open arm entries in EPM test. I, J: Time spent in the interaction zone and SI ratio in SI test. K–N: Representative tracks in OFT, EPM, and SI test (upper panel: Target-absent trial; lower panel: Target-present trial). Data are presented as mean±SEM, analyzed by one-way ANOVA. n=8 in each group; *: P<0.050; **: P<0.010. EPM: Elevated plus maze test; OFT: Open-field test; SEM: Standard error of the mean; SI: Social interaction.

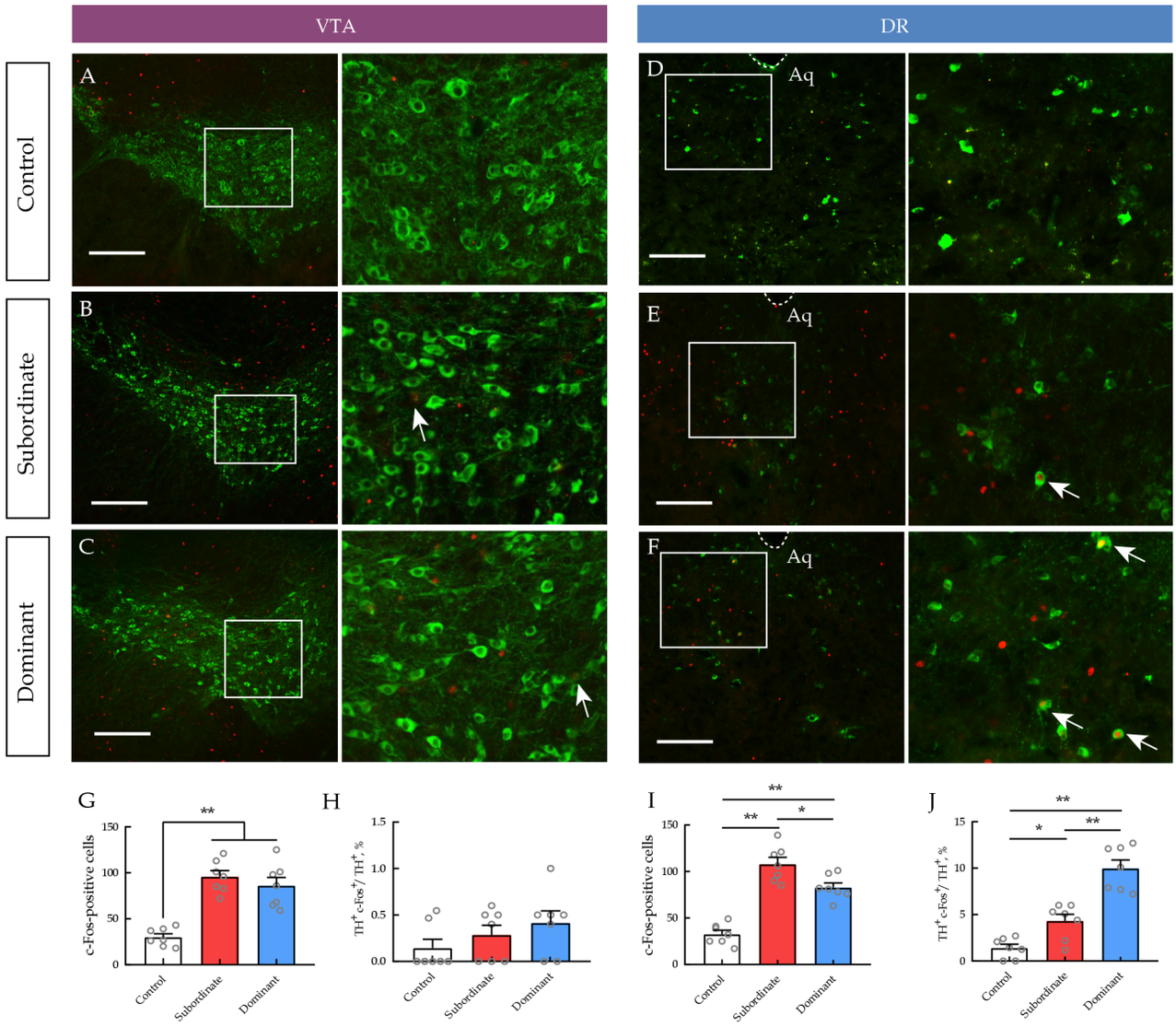

Figure 2 TH and c-Fos colocalization in the VTA and DR

A–F: Representative immunofluorescent images of c-Fos$^+$ (red dots) and TH$^+$ neurons (green cells) in the VTA and DR. White squares indicate position where the right column images were taken and arrows indicate double-labeled cells. Scale bars: 100 μm. G–J: Quantification of c-Fos and TH/c-Fos colocalization in the VTA and DR. Data are presented as mean±SEM, analyzed by one-way ANOVA. n=7 in each group. *: P<0.050; **: P<0.010. Aq: Aqueduct; DR: Dorsal raphe nucleus; SEM: Standard error of the mean; TH: Tyrosine hydroxylase; VTA: Ventral tegmental area.

Subsequent behavioral assays revealed selective effects on anxiety-like measures. In dominant mice, hM4D(Gi)-mediated inhibition significantly reduced time spent in the open arms in the EPM (Figure 5L, $F_{(2,21)}$=5.112, P=0.016; hM4D(Gi): Veh vs. CNO, P=0.047) and decreased the SI ratio in the SI test (Figure 5M, $F_{(2,21)}$=3.566, P=0.046; hM4D(Gi): Veh vs. CNO, P=0.013). In subordinate mice, hM3D(Gq)-mediated activation significantly increased time spent in the open arms in the EPM (Figure 5P, $F_{(2,21)}$=9.245, P<0.01; hM3D(Gq): Veh vs. CNO, P=0.021) but did not significantly affect the SI ratio in the SI test (Figure 5Q, $F_{(2,21)}$=0.311, P=0.736). Notably, these treatments did not significantly alter behavioral performance of either dominant or subordinate mice in the OFT (Figure 5J: $F_{(2,21)}$=1.375, P=0.275; Figure 5K: $F_{(2,21)}$=2.389, P=0.116; Figure 5N: $F_{(2,21)}$=1.308, P=0.319; Figure 5O: $F_{(2,21)}$=2.793, P=0.084). These findings indicate that while VTA DA neuron modulation does not significantly influence social rank, it can alter specific anxiety-related behaviors in a rank-dependent manner.

Inhibition of DR DA neurons lowers dominant rank and sociability, whereas activation of DR DA neurons increases subordinate rank and reduces anxiety

Targeted chemogenetic manipulations were next applied to DR DA neurons (Figure 6A). Validation of the viral strategy is provided in Supplementary Figure S4C, D, G, H. In the tube test, hM4D(Gi)-mediated inhibition of DR DA neurons in dominant mice significantly reduced their social rank (hM4D(Gi)+Veh vs. hM4D(Gi)+CNO, rank change rate: 62.5%, Fisher's exact test, P=0.026, Figure 6F). Conversely, hM3D(Gq)-mediated activation in subordinate mice significantly increased their social rank (hM3D(Gq)+Veh vs. hM3D(Gq)+CNO, rank change rate: 75%, Fisher's exact test, P<0.010, Figure 6H). Subsequent behavioral assays revealed that activation of DR DA neurons in subordinates significantly increased time spent in the open arms of the EPM (Figure 6P, $F_{(2,21)}$=9.303, P<0.01; hM3D(Gq): Veh vs. CNO, P=0.031), indicating reduced anxiety-like behavior. However, inhibition of DR DA neurons significantly reduced their SI ratio in the SI test

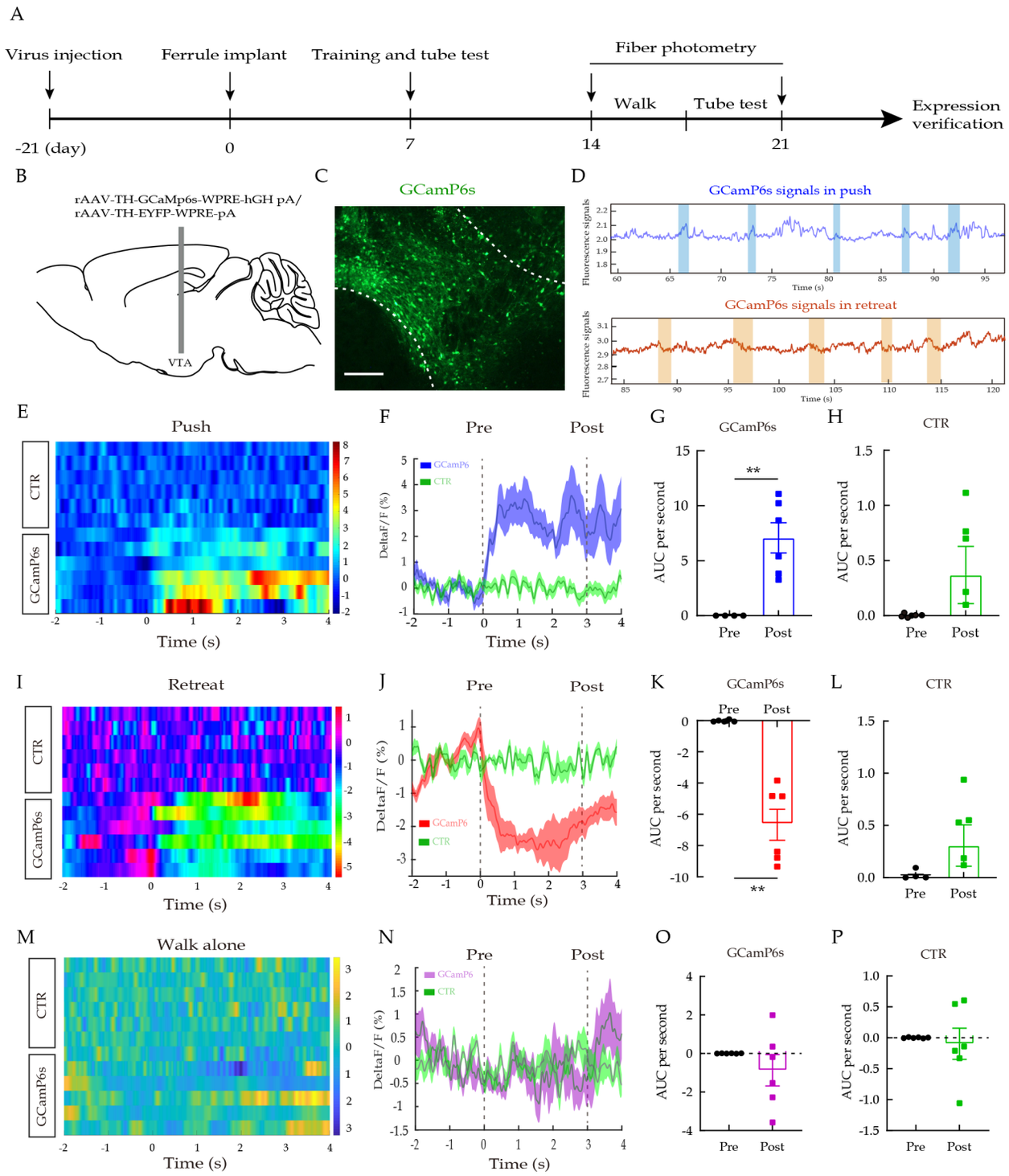

Figure 3 Fiber photometry recordings of VTA DA neurons during tube test

A: Study timeline. B: Viral injection strategy. C: Histology showing expression of GCaMP6s. Scale bar: 100 μm. D: Representative fluorescence changes of GCaMP6s during push and retreat. E, F, I, J, M, N: Heatmaps and peri-event plots of fluorescence signals aligned to onsets of push (E, F), retreat (I, J), and walk alone (M, N) in mice expressing GCaMP6s and control eGFP virus. In heatmap, different color bars represent different mice. In peri-event plot, line denotes mean signals of behaviors; shaded region denotes SE. n=18–24 trials from six mice. G, H, K, L, O, P: Quantification of changes in fluorescence signals before and after events in mice expressing GCaMP6s and control eGFP virus (G, H: Push; K, L: Retreat; O, P: Walk alone). Data are presented as mean±SEM, analyzed by paired t test. **: P<0.010. CTR: Control; DA: Dopamine; SEM: Standard error of the mean; TH: Tyrosine hydroxylase; VTA: Ventral tegmental area.

(Figure 6Q, $F_{(2,21)}$=7.297, P<0.01; hM4D(Gi): Veh vs. CNO, P=0.045). OFT performance was unaffected by either activation or inhibition of DR DA neurons in both dominant and subordinate mice (Figure 6J: $F_{(2,21)}$=2.836, P=0.081; Figure 6K: $F_{(2,21)}$=0.352, P=0.707; Figure 6N: $F_{(2,21)}$=0.362, P=0.701; Figure 6O: $F_{(2,21)}$=2.349, P=0.120). These findings identify DR DA neurons as critical modulators of both social rank and specific socio-emotional behaviors in a rank-dependent manner.

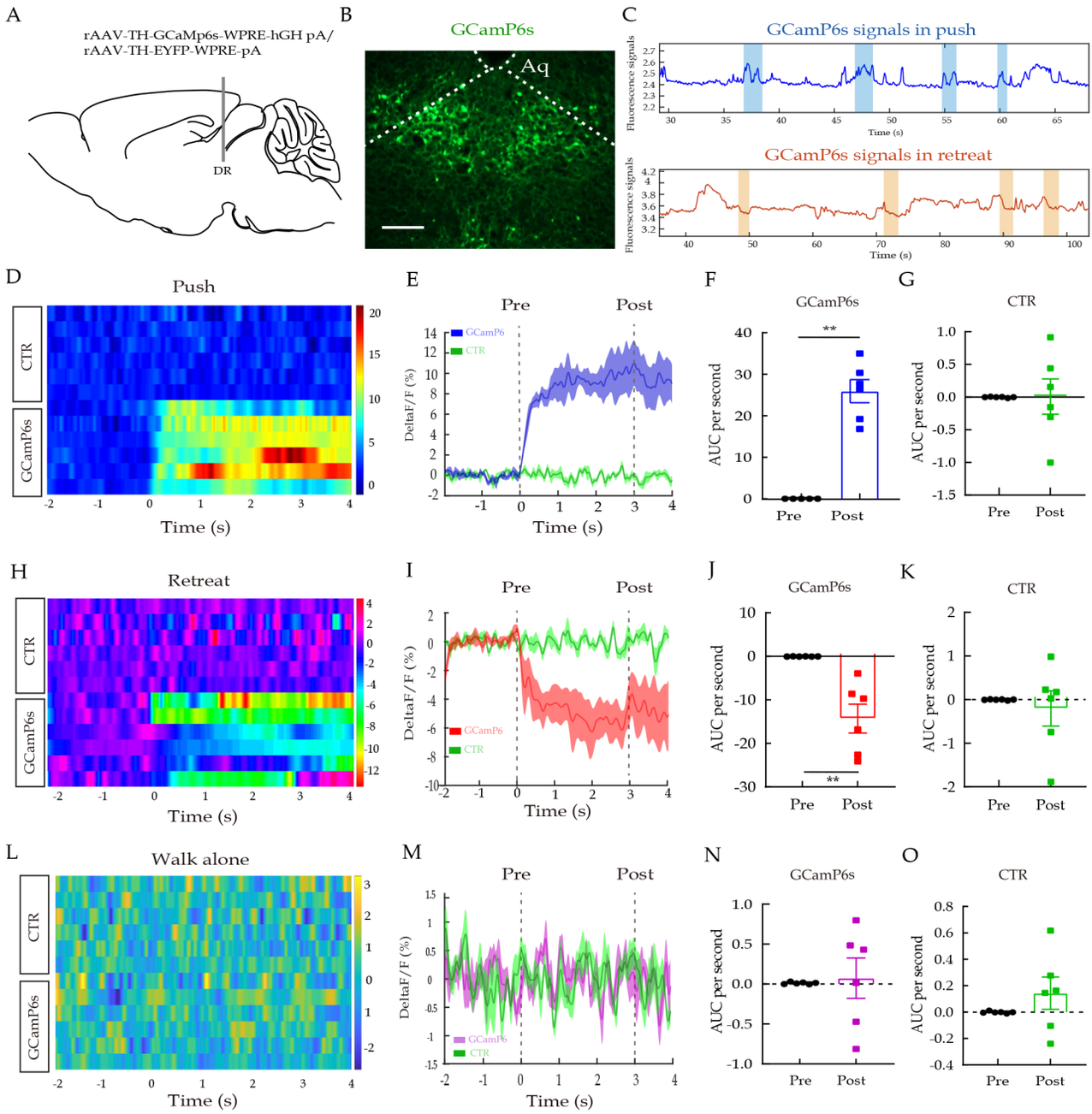

Figure 4 Fiber photometry recordings of DR DA neurons during tube test

A: Viral injection strategy. B: Histology showing expression of GCaMP6s. Scale bar: 100 μm. C: Representative fluorescence changes of GCaMP6s during push and retreat. D, E, H, I, L, M: Heatmaps and peri-event plots of fluorescence signals aligned to onsets of push (D, E), retreat (H, I), and walk alone (L, M) in mice expressing GCaMP6s and control eGFP virus. In heatmap, different color bars represent different mice. In peri-event plot, line denotes mean signals of behaviors; shaded region denotes SE. *n*=17–25 trials from six mice. F, G, J, K, N, O: Quantification of changes in fluorescence signals before and after events in mice expressing GCaMP6s and control eGFP virus (F, G: Push; J, K: Retreat; N, O: Walk alone). Data are presented as mean±SEM, analyzed by paired *t* test. **: *P*<0.010. CTR: Control; DA: Dopamine; DR: Dorsal raphe nucleus; SEM: Standard error of the mean; TH: Tyrosine hydroxylase.

DISCUSSION

This study delineated the distinct contributions of VTA and DR DA neurons to the regulation of social rank in mice. Through c-Fos profiling and fiber photometry, DR DA neurons in dominant mice exhibited heightened activity both during and following social encounters. Chemogenetic manipulation of these neurons bidirectionally altered dominance rank, establishing a direct causal role. In contrast, manipulation of VTA DA neurons failed to produce comparable effects, highlighting the region-specificity of dopaminergic circuits in social hierarchy regulation. These findings position DR DA neurons, rather than VTA DA neurons, as a critical node in the neural architecture underlying social dominance in mice.

Consistent with previous studies (Battivelli et al., 2024b; Jiang et al., 2023; Xin et al., 2025; Xing et al., 2022; Zhang et al., 2022; Zhou et al., 2017), male C57BL/6 mice formed linear social hierarchies within a few days of co-housing (Figure 1C, D). Across behavioral assays, no significant rank-dependent differences were detected in anxiety-like behaviors or sociability (Figure 1E–J), aligning with findings from several

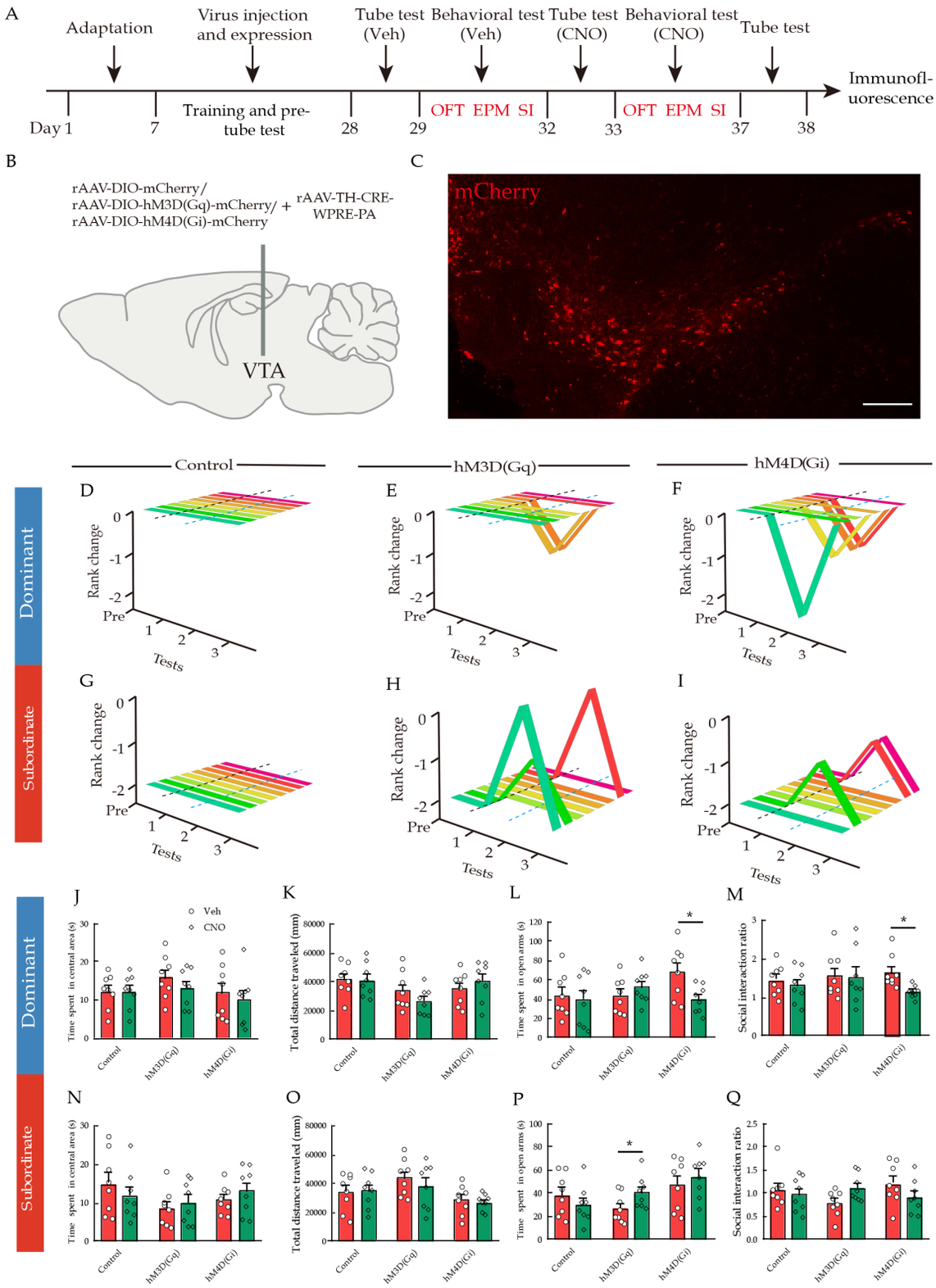

Figure 5 Chemogenetic modulation of VTA TH$^+$ neurons

A: Study timeline. B: Viral injection strategy. C: Immunohistochemical image showing DREADD expressions in the VTA, scale bar: 100 μm. D–I: Summary of rank changes in dominant (D–F) and subordinate (G–I) individuals. J, K, N, O: Time spent in the central zone and total distance traveled by dominant (J, K) and subordinate (N, O) individuals in OFT. L, P: Time spent in open arms by dominant (L) and subordinate (P) individuals in EPM. M, Q: SI ratio in dominant (M) and subordinate (Q) individuals in the three-chamber test. Data are presented as mean±SEM. n=8 in each group. *: P<0.050. Data in graph "D–I" analyzed by Fishers exact test, "J–Q" analyzed by two-way repeated-measures ANOVA. SI ratio: Social interaction ratio. CNO: Clozapine *N*-oxide; DREADDs: Designer receptors exclusively activated by designer drugs; EPM: Elevated plus maze test; OFT: Open-field test; SEM: Standard error of the mean; SI: Social interaction; TH: Tyrosine hydroxylase; Veh: Vehicle; VTA: Ventral tegmental area.

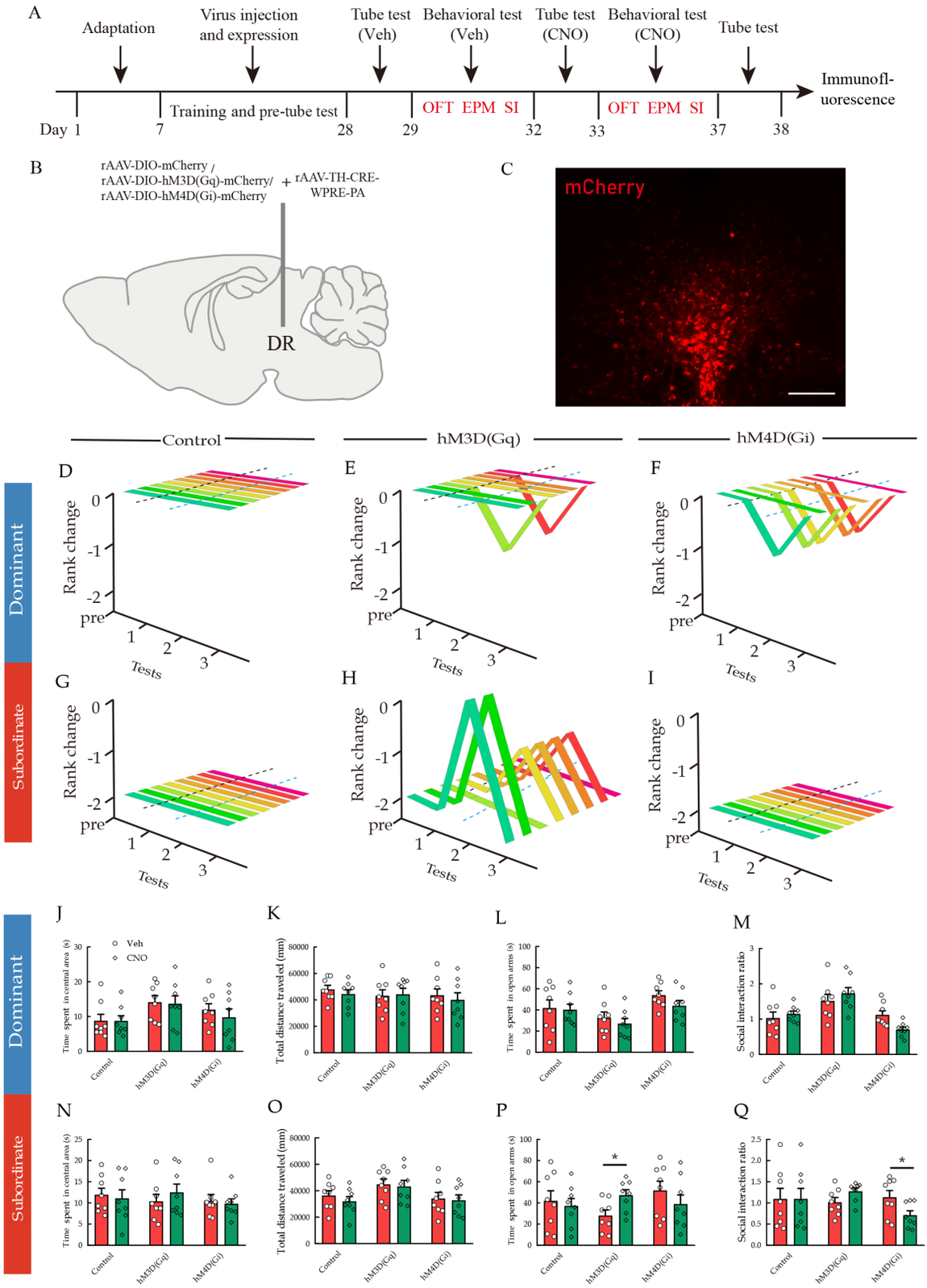

Figure 6 Chemogenetic modulation of DR TH⁺ neurons

A: Study timeline. B: Viral injection strategy. C: Immunohistochemical image showing DREADD expressions in the DR, scale bar: 100 μm. D–I: Summary of rank changes in dominant (D–F) and subordinate (G–I) individuals. J, K, N, O: Time spent in central zone and total distance traveled by dominant (J, K) and subordinate (N, O) individuals in OFT. L, P: Time spent in open arms by dominant (L) and subordinate (P) individuals in EPM. M, Q: SI ratio in dominant (M) and subordinate (Q) individuals in the three-chamber test. Data are presented as mean±SEM. *n*=8 in each group; *: *P*<0.050. Data in graph "D–I" analyzed by Fishers exact test, "J–Q" analyzed by two-way repeated-measures ANOVA. SI ratio: Social interaction ratio. CNO: Clozapine *N*-oxide; DR: Dorsal raphe nucleus; DREADDs: Designer receptors exclusively activated by designer drugs; EPM: Elevated plus maze test; OFT: Open-field test; SEM: Standard error of the mean; SI: Social interaction; TH: Tyrosine hydroxylase; Veh: Vehicle.

studies (Jiang et al., 2023; Varholick et al., 2018, 2021). However, other investigations have reported rank-related differences, with dominants exhibiting either increased (Battivelli et al., 2024b; Larrieu et al., 2017) or decreased anxiety (Horii et al., 2017; Song et al., 2023) and enhanced sociability (Kunkel & Wang, 2018; Li et al., 2023; Šabanović et al., 2020) compared to subordinates. Such discrepancies may reflect the inherent variability of behavioral phenotypes (Varholick et al., 2018, 2021), which are highly sensitive to external environments and physiological factors, such as test apparatus, light cycles, rearing conditions, and animal strains.

Dopaminergic signaling has long been implicated in social competition (Ghosal et al., 2019; Rillich & Stevenson, 2014), yet the specific contribution of VTA DA neurons remains a subject of debate. Optogenetic stimulation of VTA DA neurons has been shown to induce dominant behavior during competition for rewards (Lozano-Montes et al., 2019), and enhanced VTA DA activity via disinhibition has been linked to higher social dominance in rats (van der Kooij et al., 2018). In contrast, research has also shown that VTA DA neurons exhibit lower activity in dominant mice, with chemogenetic inhibition increasing social rank (Battivelli et al., 2024b). Similarly, in male mice, mPFC-NAc projections are reported to drive social winning, while mPFC-VTA projections promote social defeat (Choi et al., 2024). In the present study, VTA DA neurons exhibited phasic activation during active push behaviors and suppression during passive retreats in the tube test (Figure 3), yet chemogenetic manipulation of these neurons did not significantly affect social dominance (Figure 5). Moreover, c-Fos immunolabeling did not reveal increased VTA DA activity in dominant mice (Figure 2). These conflicting results may arise from methodological differences or selective targeting of distinct DA neuron subpopulations, which differ in molecular identity, connectivity, and functional specialization (Lammel et al., 2008). Future studies integrating subpopulation-specific targeting with *in vivo* single-unit recording may help resolve these circuit-level discrepancies.

Accumulating evidence suggests that DR DA neurons form a specialized midbrain DA subsystem, playing important regulatory roles in memory expression, opioid addiction, loneliness, depression, and arousal (Lin et al., 2021; Matthews et al., 2016; Wang et al., 2024). In the current study, DR DA neurons in dominant mice displayed heightened activity both during and after social competition in the tube test (Figure 2, Figure 4). Chemogenetic activation or inhibition of these neurons bidirectionally shifted dominance rank (Figure 6), providing direct causal evidence for their role in hierarchy regulation. Similarly, Xin et al. (2025) reported that stimulation of mPFC-DR projections promotes competitive success in the tube test, suggesting that DR DA neurons may be downstream targets of this pathway. However, verification of this hypothesis will require targeted connectivity analyses, such as monosynaptic tracing or cell-type-specific electrophysiology, to determine whether mPFC inputs directly engage DR DA neurons. Additionally, given that the DR is a principal serotonergic hub, the potential involvement of 5-HT or other neuronal types cannot be excluded, particularly in light of evidence that mPFC projections preferentially innervate 5-HTergic populations (Weissbourd et al., 2014). Furthermore, whether baseline DR DA activity differs between dominant and subordinate individuals remains unclear—a question that could be resolved through *in vivo* electrophysiological recordings in freely behaving animals.

Manipulation of VTA and DR DA neurons also modulated anxiety-like and social behaviors. In the EPM test, VTA DA inhibition increased anxiety-like behavior and reduced sociability, particularly in dominant individuals (Figure 5L, M), whereas activation produced an anxiolytic effect (Figure 5P). These findings are consistent with previous studies on VTA DA neurons (Bariselli et al., 2018; Zweifel et al., 2011). For DR DA neurons, chemogenetic activation increased open-arm exploration in subordinates during the EPM test (Figure 6P), consistent with reduced anxiety-like behavior, whereas inhibition decreased the SI ratio (Figure 6Q). In contrast, manipulation of DR DA neurons did not significantly alter anxiety or sociability in dominant individuals (Figure 6L, M). Prior studies reveal similarly complex and context-dependent effects: Taylor et al. (2019) reported that DR DA activation produced profound analgesia without changes in anxiety, while Matthews et al. (2016) found that optogenetic activation induced a loneliness-like state that enhanced sociability in the three-chamber test, with photoinhibition producing the opposite effect. These observed discrepancies suggest that social experience, particularly hierarchical status, may strongly influence the behavioral outcomes of DR DA neuron manipulation, potentially reshaping their functional role in socio-emotional processing.

Unlike VTA DA neurons which send extensive projections to the limbic and cortical regions, DR DA neurons display a more restricted projection pattern, primarily targeting the CeA and BNST (Lin et al., 2020). This anatomical distinction underscores the need for future studies to delineate the precise neural pathways underlying social hierarchy formation. Furthermore, DA is known to exert its effects via two major receptor subtypes, D1-like (D1Rs) and D2-like (D2Rs), which differ in intracellular signaling cascades and functional outcomes (Li et al., 2023; Liu et al., 2021). Systematic investigation of their respective contributions to social dominance within downstream projection targets is also warranted.

Our immunofluorescence analyses revealed significant c-Fos activation in both the VTA and DR following tube test-based social competition in dominant and subordinate mice (Figure 2G, I). Double-labeling analyses further demonstrated that c-Fos activation was selectively elevated in DR DA neurons of dominant individuals (Figure 2J) but not in VTA DA neurons of either rank group (Figure 2H). Given that c-Fos is a broad marker of neuronal activity and does not necessarily correlate with specific behavioral outputs, these findings suggest that other neuronal types may also contribute to social competition-related behaviors, including anxiety-like responses—a hypothesis that merits targeted investigation in future studies.

Overall, the current study identified DR DA neurons as key modulators of social hierarchy in mice. Nevertheless, several limitations should be noted. First, although the majority of virally transduced cells were TH^+, potential off-target infection of other neuronal populations cannot be excluded as a confounding variable. Second, social dominance was not corroborated using complementary behavioral paradigms, such as the warm spot or scent-marking tests, despite the tube test being extensively validated for this purpose in previous studies (Fan et al., 2019; Larrieu et al., 2017). Furthermore, considering the current gap between neuroscience and ethology (Battivelli et al., 2024a; Murlanova et al., 2022), future studies should incorporate more

ethologically relevant approaches, such as employing wild-derived strains and determining dominant-subordinate relationships under semi-natural conditions over extended time periods, to better validate and contextualize the findings. Third, the study was conducted in triads of male mice, leaving the generalizability of these findings to larger groups or female cohorts unresolved. Finally, although chemogenetic modulation of social rank produced more robust effects in the DR, some individuals also exhibited changes following VTA modulation. Studies with larger sample sizes may yield different conclusions. Despite these limitations, this study provides new insights into the neurochemical mechanisms governing social dominance.

SUPPLEMENTARY DATA

Supplementary data to this article can be found online.

COMPETING INTERESTS

The authors declare that they have no competing interests.

AUTHORS' CONTRIBUTIONS

L.F.L., F.D.T., and Z.X.H. participated in study design. Y.J.L. and B.L.S. conducted most experiments and wrote the original draft. Q.A. participated in fiber photometry recording experiments. J.T., L.R., Y.H.S., J.W.W. and J.Z. participated in behavioral experiments and data collection and analysis. All authors read and approved the final version of the manuscript.

REFERENCES

Amaral IM, Hofer A, El Rawas R. 2021. Is it possible to shift from down to top rank? A focus on the mesolimbic dopaminergic system and cocaine abuse. *Biomedicines*, **9**(8): 877.

Bariselli S, Hörnberg H, Prévost-Solié C, et al. 2018. Role of VTA dopamine neurons and neuroligin 3 in sociability traits related to nonfamiliar conspecific interaction. *Nature Communications*, **9**(1): 3173.

Battivelli D, Fan ZX, Hu HL, et al. 2024a. How can ethology inform the neuroscience of fear, aggression and dominance?. *Nature Reviews Neuroscience*, **25**(12): 809–819.

Battivelli D, Vernochet C, Conabady E, et al. 2024b. Dopamine neuron activity and stress signaling as links between social hierarchy and psychopathology vulnerability. *Biological Psychiatry*, **95**(8): 774–784.

Cho JR, Treweek JB, Robinson JE, et al. 2017. Dorsal raphe dopamine neurons modulate arousal and promote wakefulness by salient stimuli. *Neuron*, **94**(6): 1205–1219. e8.

Choi TY, Jeon H, Jeong S, et al. 2024. Distinct prefrontal projection activity and transcriptional state conversely orchestrate social competition and hierarchy. *Neuron*, **112**(4): 611–627. e8.

Dwortz MF, Curley JP, Tye KM, et al. 2022. Neural systems that facilitate the representation of social rank. *Philosophical Transactions of the Royal Society B: Biological Sciences*, **377**(1845): 20200444.

Fan ZX, Chang JR, Liang YL, et al. 2023. Neural mechanism underlying depressive-like state associated with social status loss. *Cell*, **186**(3): 560–576. e17.

Fan ZX, Zhu H, Zhou TT, et al. 2019. Using the tube test to measure social hierarchy in mice. *Nature Protocols*, **14**(3): 819–831.

Garritsen O, van Battum EY, Grossouw LM, et al. 2023. Development, wiring and function of dopamine neuron subtypes. *Nature Reviews Neuroscience*, **24**(3): 134–152.

Ghosal S, Sandi C, van der Kooij MA. 2019. Neuropharmacology of the mesolimbic system and associated circuits on social hierarchies. *Neuropharmacology*, **159**: 107498.

Horii Y, Nagasawa T, Sakakibara H, et al. 2017. Hierarchy in the home cage affects behaviour and gene expression in group-housed C57BL/6 male mice. *Scientific Reports*, **7**(1): 6991.

Janet R, Ligneul R, Losecaat-Vermeer AB, et al. 2022. Regulation of social hierarchy learning by serotonin transporter availability. *Neuropsychopharmacology*, **47**(13): 2205–2212.

Jiang Y, Zhou J, Song BL, et al. 2023. 5-HT1A receptor in the central amygdala and 5-HT2A receptor in the basolateral amygdala are involved in social hierarchy in male mice. *European Journal of Pharmacology*, **957**: 176027.

Johnson SL, Leedom LJ, Muhtadie L. 2012. The dominance behavioral system and psychopathology: evidence from self-report, observational, and biological studies. *Psychological Bulletin*, **138**(4): 692–743.

Kaplan JR, Manuck SB, Fontenot MB, et al. 2002. Central nervous system monoamine correlates of social dominance in cynomolgus monkeys (*Macaca fascicularis*). *Neuropsychopharmacology*, **26**(4): 431–443.

Kunkel T, Wang HB. 2018. Socially dominant mice in C57BL6 background show increased social motivation. *Behavioural Brain Research*, **336**: 173–176.

Lammel S, Hetzel A, Häckel O, et al. 2008. Unique properties of mesoprefrontal neurons within a dual mesocorticolimbic dopamine system. *Neuron*, **57**(5): 760–773.

Larrieu T, Cherix A, Duque A, et al. 2017. Hierarchical status predicts behavioral vulnerability and nucleus accumbens metabolic profile following chronic social defeat stress. *Current Biology*, **27**(14): 2202–2210. e4.

Leclair KB, Russo SJ. 2021. Using social rank as the lens to focus on the neural circuitry driving stress coping styles. *Current Opinion in Neurobiology*, **68**: 167–180.

Li LF, Li ZL, Song BL, et al. 2023. Dopamine D2 receptors in the dorsomedial prefrontal cortex modulate social hierarchy in male mice. *Current Zoology*, **69**(6): 682–693.

Lin R, Liang JM, Luo MM. 2021. The raphe dopamine system: roles in salience encoding, memory expression, and addiction. *Trends in Neurosciences*, **44**(5): 366–377.

Lin R, Liang JM, Wang RY, et al. 2020. The raphe dopamine system controls the expression of incentive memory. *Neuron*, **106**(3): 498–514. e8.

Liu CL, Goel P, Kaeser PS. 2021. Spatial and temporal scales of dopamine transmission. *Nature Reviews Neuroscience*, **22**(6): 345–358.

Liu YJ, Jiang Y, Bai YT, et al. 2025. Serotonergic modulation of social dominance via the dorsal raphe-central amygdala circuit in male mice. *Integrative Zoology*, doi: 10.1111/1749-4877.70003.

Lozano-Montes L, Astori S, Abad S, et al. 2019. Latency to reward predicts social dominance in rats: a causal role for the dopaminergic mesolimbic system. *Frontiers in Behavioral Neuroscience*, **13**: 69.

Madigan A, Daly M. 2023. Socioeconomic status and depressive symptoms and suicidality: the role of subjective social status. *Journal of Affective Disorders*, **326**: 36–43.

Martinez D, Orlowska D, Narendran R, et al. 2010. Dopamine type 2/3 receptor availability in the striatum and social status in human volunteers. *Biological Psychiatry*, **67**(3): 275–278.

Matthews GA, Nieh EH, Vander Weele CM, et al. 2016. Dorsal raphe dopamine neurons represent the experience of social isolation. *Cell*, **164**(4): 617–631.

Murlanova K, Kirby M, Libergod L, et al. 2022. Multidimensional nature of dominant behavior: insights from behavioral neuroscience. *Neuroscience & Biobehavioral Reviews*, **132**: 603–620.

Qu C, Ligneul R, Van der Henst JB, et al. 2017. An integrative interdisciplinary perspective on social dominance hierarchies. *Trends in Cognitive Sciences*, **21**(11): 893–908.

Rillich J, Stevenson PA. 2014. A fighter's comeback: dopamine is necessary for recovery of aggression after social defeat in crickets. *Hormones and Behavior*, **66**(4): 696–704.

Šabanović M, Liu H, Mlambo V, et al. 2020. What it takes to be at the top:

The interrelationship between chronic social stress and social dominance. *Brain and Behavior*, **10**(12): e01896.

Song BL, Zhou J, Jiang Y, et al. 2023. Dopamine D2 receptor within the intermediate region of the lateral septum modulate social hierarchy in male mice. *Neuropharmacology*, **241**: 109735.

Taylor NE, Pei JZ, Zhang J, et al. 2019. The role of glutamatergic and dopaminergic neurons in the periaqueductal gray/dorsal raphe: separating analgesia and anxiety. *eNeuro*, **6**(1): ENEURO.0018–18.2019.

Tenchov R, Sasso JM, Zhou QA. 2025. Evolving landscape of parkinson's disease research: challenges and perspectives. *ACS Omega*, **10**(2): 1864–1892.

Torquet N, Marti F, Campart C, et al. 2018. Social interactions impact on the dopaminergic system and drive individuality. *Nature Communications*, **9**(1): 3081.

Uchida K, Ng R, Vydro SA, et al. 2022. The benefits of being dominant: health correlates of male social rank and age in a marmot. *Current Zoology*, **68**(1): 19–26.

van der Kooij MA, Hollis F, Lozano L, et al. 2018. Diazepam actions in the VTA enhance social dominance and mitochondrial function in the nucleus accumbens by activation of dopamine D1 receptors. *Molecular Psychiatry*, **23**(3): 569–578.

Varholick JA, Bailoo JD, Jenkins A, et al. 2021. A systematic review and meta-analysis of the relationship between social dominance status and common behavioral phenotypes in male laboratory mice. *Frontiers in Behavioral Neuroscience*, **14**: 624036.

Varholick JA, Bailoo JD, Palme R, et al. 2018. Phenotypic variability between Social Dominance Ranks in laboratory mice. *Scientific Reports*, **8**(1): 6593.

Wang WT, Wang D, Zhao D, et al. 2024. Dorsal raphe dopaminergic neurons target CaMKII$^+$ neurons in dorsal bed nucleus of the stria terminalis for mediating depression-related behaviors. *Translational Psychiatry*, **14**(1): 408.

Wang Y, Jiang Y, Song BL, et al. 2022. mGlu2/3 receptors within the ventral part of the lateral septal nuclei modulate stress resilience and vulnerability in mice. *Brain Research*, **1779**: 147783.

Weissbourd B, Ren J, DeLoach KE, et al. 2014. Presynaptic partners of dorsal raphe serotonergic and GABAergic neurons. *Neuron*, **83**(3): 645–662.

Xin QH, Zheng DY, Zhou TT, et al. 2025. Deconstructing the neural circuit underlying social hierarchy in mice. *Neuron*, **113**(3): 444–459. e7.

Xing B, Mack NR, Zhang YX, et al. 2022. Distinct roles for prefrontal dopamine D1 and D2 neurons in social hierarchy. *The Journal of Neuroscience*, **42**(2): 313–324.

Zhang CY, Zhu H, Ni ZY, et al. 2022. Dynamics of a disinhibitory prefrontal microcircuit in controlling social competition. *Neuron*, **110**(3): 516–531. e6.

Zhou J, Wu JW, Song BL, et al. 2024. 5-HT1A receptors within the intermediate lateral septum modulate stress vulnerability in male mice. *Progress in Neuro-Psychopharmacology and Biological Psychiatry*, **132**: 110966.

Zhou TT, Sandi C, Hu HL. 2018. Advances in understanding neural mechanisms of social dominance. *Current Opinion in Neurobiology*, **49**: 99–107.

Zhou TT, Zhu H, Fan ZX, et al. 2017. History of winning remodels thalamo-PFC circuit to reinforce social dominance. *Science*, **357**(6347): 162–168.

Zweifel LS, Fadok JP, Argilli E, et al. 2011. Activation of dopamine neurons is critical for aversive conditioning and prevention of generalized anxiety. *Nature Neuroscience*, **14**(5): 620–626.